

Measuring and modeling drillstring vibrations with top drive and near-bit sensors

Anton Egorov, Pavel Golikov (Aramco Moscow Research Center), Ilya Silvestrov, Andrey Bakulin (Saudi Aramco, EXPEC Advanced Research Center), Flavio Poletto, Biancamaria Farina (OGS – Istituto Nazionale di Oceanografia e di Geofisica Sperimentale, Ts, Italy)

Summary

In drill-bit generated seismic, understanding propagation of drillstring vibrations is a key factor for successful processing and interpretation. These vibrations are measured by the pilot sensors located at the top drive or down hole. Different sensor positions in the drillstring give rise to distinct drillstring-related arrivals. Using a unique dataset that contains recordings of both top drive and downhole sensors, we conduct a modelling-based analysis of the vibrations recorded in the first DrillCAM field trial. We analyze the extensional waves recorded on the vertical component and identify the main drillstring-related multiple waves recorded on the top drive and downhole signal autocorrelations. We also analyze the dependence of the top drive signal on the type of drilling bit by comparing the records from roller-cone and polycrystalline diamond compact (PDC) bits. While PDC bits tend to produce relatively weak signals at depth, we observe notable exceptions.

Introduction

Since the second half of the 20th century, various attempts have been made to use the vibrations of the drill bit for the reconstruction of the subsurface properties and/or estimation of the drilling conditions. In seismic-while-drilling (SWD) operations, the drill bit is used as a seismic source, and its vibrations are recorded by surface seismic sensors or downhole sensors in another well. To obtain the signature of the drill-bit source, additional pilot seismic sensors are placed near the top (usually mounted on the top drive) or the bottom (near the bit) of the drillstring (Poletto and Miranda, 2004). Vibrations recorded by these sensors can also be directly used for identification of boundaries between the formations while drilling (Myers et al., 2002). In addition to the direct arrivals from the bit, the data recorded by these pilot sensors contain multiples and reverberations due to the boundaries between different parts of the bottomhole assembly (BHA) and the segments of the drillstring (Poletto et al., 2001).

We analyze the autocorrelations of the data recorded by the top drive and downhole sensors and compare them to the drillstring wave propagation modelling results, identifying main recorded events. These signals are used as a pilot for SWD analysis (Poletto and Miranda, 2004). They also can be applied to characterize drilling malfunctions and formation properties. We perform a comparative analysis of the events recorded by the top drive and downhole sensors. In most cases, the top drive pilot sensor is utilized in the

SWD processing and the analysis of vibrations, since it is easier to deploy, and its recordings are available in real-time, as opposed to the downhole sensor, that can transmit real-time high-frequency data only when fast wired-pipe telemetry is used. The top drive and downhole datasets contain different patterns of drillstring-related arrivals caused by many boundaries inside the drillstring generating interfering reflected and transmitted waves, as well as superimposed local vibrations due to drillpipe-borehole interactions. Understanding this complex propagation is critical in any application that relies on using these vibrations, from SWD to formation property estimation.

We utilize top drive and downhole sensor recordings acquired during a recent onshore field trial of the DrillCAM system (Bakulin et al., 2019). Recordings of the top drive and downhole sensors were simultaneously acquired from the surface to the depth of 10,000 ft along with surface measurements using wireless geophones. Roller-cone and polycrystalline diamond compact (PDC) bits were used for drilling this well. This study focuses on understanding the propagation of extensional drillstring signals as a function of bit depth and bit type, as it is known that PDC drilling may produce unfavorable signal-to-noise ratios for SWD (Naville et al., 2004).

Method

To model wave propagation in the drillstring, we apply a transmission line/matrix propagator algorithm following the approach proposed by Poletto et al. (2001). The algorithm takes dimensions and weights of the BHA and the drillpipes as input data and generates seismic wavefields (extensional mode) at receiver locations of interest (such as at the top drive and near the bit) or their autocorrelations. We use a zero-phase wavelet with characteristic trapezoidal frequencies of 6-10-80-100 Hz.

Field top drive recordings from the vertical component were obtained as 30-second-long segments, autocorrelated and stacked over one drillpipe length (30 ft) to increase the signal-to-noise ratio. Averaging over a period of constant drillstring length allows to keep all arrivals including multiples at the same time lags for coherent stacking. The relation between the drilling time and depth is taken from the electronic drilling parameter recorder. For the downhole sensor, we conduct the same processing, but we average over 60 ft to further increase the signal-to-noise ratio.

Measuring and modeling drillstring vibrations

Examples– Analysis of top drive autocorrelations

Poletto et al. (2014) interpret different BHA-related events in synthetic and field drill-bit signals from surface and downhole pilot sensors. Here, we apply a similar analysis. Before analyzing the wavefield in the top drive field data, we choose to inspect the different types of drillstring-related multiples on the synthetic top drive autocorrelations. Figure 1 shows a synthetic gather (left) and ray paths (right) for the main wave types. Two types of multiples can be identified. The first type has a constant lag for all drillstring lengths – these are the interlayer multiples (peg-legs) in one of the parts of the BHA (orange). The second type has a lag that changes linearly with increasing drillstring length (green). These are multiples of different orders that bounce between the top drive and the bit or between the top drive and the top of the BHA. Apparent velocities V_{app}^n of the multiples on these autocorrelation plots are equal to $V_{pipe}/2n$, where n is the multiple order and V_{pipe} is the drillstring effective velocity (estimated from the data as 15,960 ft/s and agreeing with calculated velocity for a periodic model using drillpipe/connector parameters and steel properties in a low-frequency approximation (Drumheller and Knudsen, 1995)).

Figure 2 compares the synthetic and field top drive deconvolved autocorrelations with the main multiples highlighted (as in Figure 1, their apparent velocities are also specified). The arrival times of these multiples are similar for the field and synthetic gathers suggesting that observed arrivals are indeed related to boundaries in the BHA. The close-up view in Figure 3 shows that the modelling replicates even the small-scale properties of the wavefield.

Notice the change in the lag between two reverberations from 50 ms to 80 ms. This lag change occurs between two different drilling runs 4 and 5, and is caused by different BHA configurations between these two runs. The length of BHA together with heavy-weight drill pipes section for Run 4 is longer (1414 vs 1250 ft), causing an earlier arrival of the first multiple between top drive and top of the BHA. This multiple is identified as a dashed green line in Figure 3, whereas its path is similar to the multiple identified by a dashed green line in Figure 1.

In Figure 2a, for all the sections acquired with the PDC bit starting from approximately 6200 ft, the field autocorrelations contain no interpretable multiples and are dominated by noise. The horizontal events seen below 6200 ft are not explained by the modelling, they may be related to the surface vibrations, which are amplified by the deconvolution. On the synthetic gather, the multiples are present; however, they have low amplitudes, and the autocorrelation values near zero time are also lower, though not seen in Figure 2. It has been reported by various authors that PDC bits produce much weaker signal compared to the roller-cone bits (Poletto and Miranda, 2004; Naville et al., 2004), limiting their applicability in SWD. This could be the primary explanation for weak signal below 6200 ft; however, there is a previous drilling run with a PDC bit at 4180-5246 ft that exhibits quite high signal-to-noise ratio, which is comparable to roller-cone data. Signal strength is further confirmed by good-quality SWD obtained with surface geophones after correlation with top drive signal from PDC at 4180-5246 ft. As such, the bit type alone may not be the only reason for the observed behavior. Another possible explanation for such a difference in the recordings could be the presence of the measurement-while-drilling

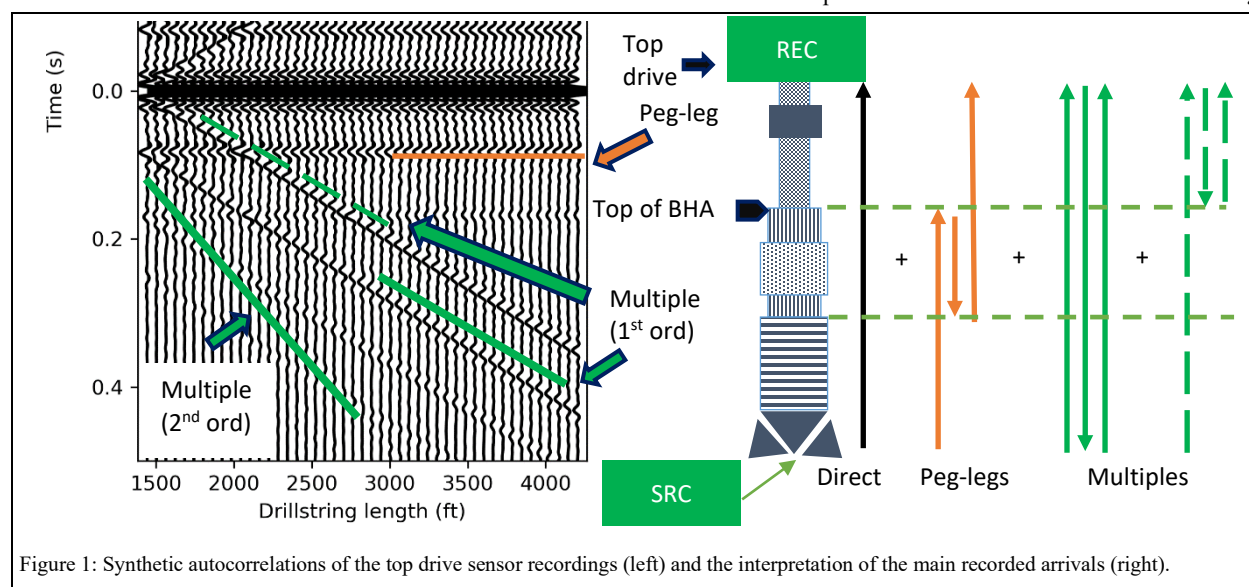


Figure 1: Synthetic autocorrelations of the top drive sensor recordings (left) and the interpretation of the main recorded arrivals (right).

Measuring and modeling drillstring vibrations

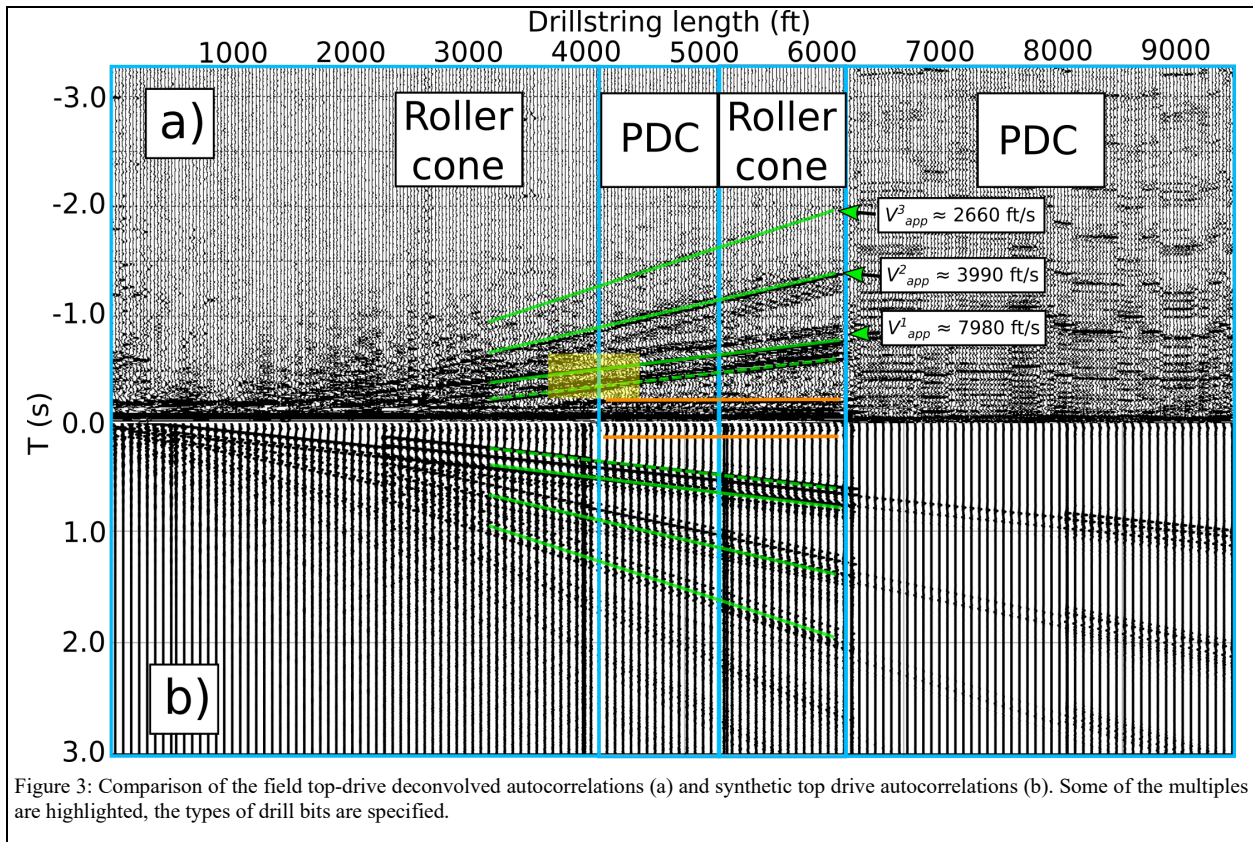


Figure 3: Comparison of the field top-drive deconvolved autocorrelations (a) and synthetic top drive autocorrelations (b). Some of the multiples are highlighted, the types of drill bits are specified.

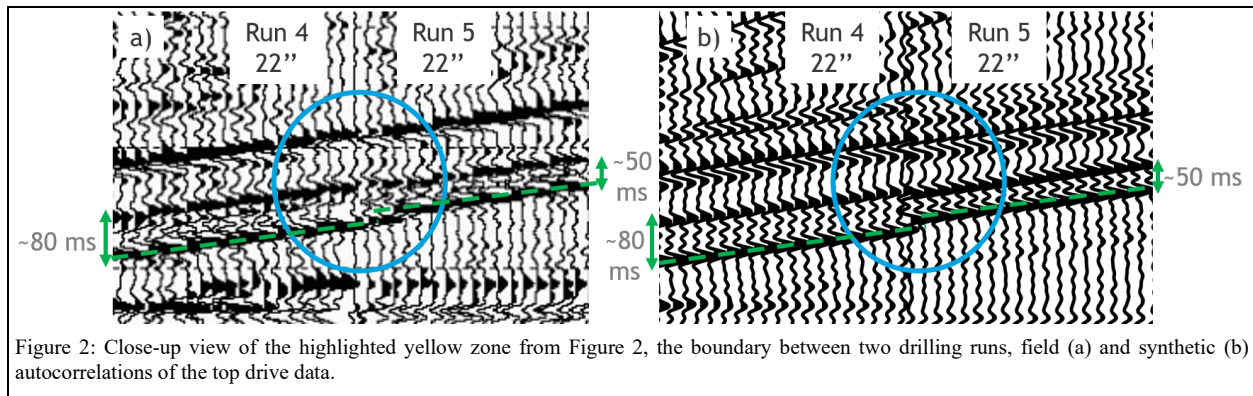


Figure 2: Close-up view of the highlighted yellow zone from Figure 2, the boundary between two drilling runs, field (a) and synthetic (b) autocorrelations of the top drive data.

(MWD) tool and the multiple activation bypass system appearing from 6200 ft – these additional segments of the BHA may further attenuate the vibrations preventing them from reaching the top drive sensor.

Examples– Analysis of downhole autocorrelations

In Figure 4, we present the experimentally observed autocorrelations obtained using the downhole sensor in the

depth interval of 700-2500 ft. We observe multiple arrivals similar, but not identical to those seen on the autocorrelations of the top drive sensor. Since the sensor is now located very close to the source, the moveout and interpretation of these multiples is different. For early arrivals, the lag does not change with increasing length of the drillstring, suggesting that these are reflections from different boundaries in the BHA and their multiples (orange). Since the BHA remains fixed, while new drillpipe

Measuring and modeling drillstring vibrations

is added at the top, these arrivals remain at the same time lag. For later arrivals, the lag increases linearly with depth, which means that these are the reflections from the top drive boundary and their multiples (green) travelling over the entire drillstring length. Reasonable agreement between arrival times and wavefields of modelled and observed vibrations suggests that we are capturing the main features of wave propagation in the drillstring.

Conclusions

Analysis of the top drive and downhole sensor autocorrelations is key to understand the drillstring vibration and perform the quality control of SWD data. We modelled the top drive and downhole pilot autocorrelations for the BHA configurations used during drilling and compared them to the field data acquired during the first DrillCAM trial on an onshore well using roller-cone and PDC bits. The main events on both datasets recorded with downhole and top drive sensors were successfully identified. We were able to reproduce similar wavefields using a transmission line modelling approach with realistic parameters for the drillstring and BHA. This modelling capability is important for real-time QC of drill-bit signals in seismic-while-drilling. Top drive field autocorrelations reveal little axial vibration energy for almost all the sections drilled by the PDC bit, except for one drilling run. One possible reason for such behavior is the introduction of an MWD tool and a multiple activation bypass system above the BHA, which may have attenuated the vibrations. In future studies, we plan to conduct further analysis of the horizontal components from top drive and downhole sensors to obtain additional insight into the radiation patterns of different bits.

Acknowledgments

The authors acknowledge T. Zharnikov, M. Al-Ali (Aramco Research Center Moscow), A. Sena and E. Hemyari (Saudi Aramco) for productive discussions on this research topic. Authors also thank Fabio Meneghini, Franco Zgauc, and Andrea Schleifer (OGS) for their support in the preparation of surface and downhole data.

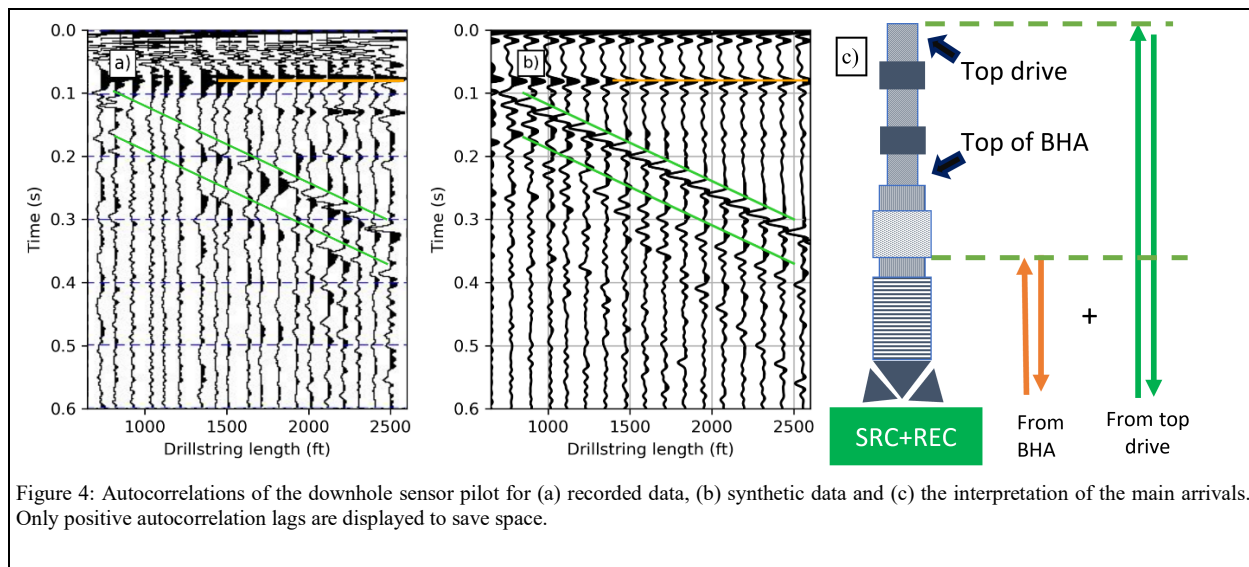


Figure 4: Autocorrelations of the downhole sensor pilot for (a) recorded data, (b) synthetic data and (c) the interpretation of the main arrivals. Only positive autocorrelation lags are displayed to save space.

REFERENCES

- Bakulin, A., E. Hemyari, and I. Silvestrov, 2019, Acquisition trial of DrillCAM: Real-time seismic with wireless geophones, instrumented top drive and near-bit accelerometer: 89th Annual International Meeting, SEG, Expanded Abstracts, 157–161, doi: <https://doi.org/10.1190/segam2019-3214516.1>
- Drumheller, D. S., and S.D. Knudsen, 1995, The propagation of sound waves in drill strings: The Journal of the Acoustical Society of America, **97**, 2116–2125, doi: <https://doi.org/10.1121/1.412004>.
- Myers, G., D. Goldberg, and J. Rector, 2002, Drill string vibration: A proxy for identifying lithologic boundaries while drilling, in J. F. Casey and D. J. Miller, eds., Proceedings of the Ocean Drilling Program, Scientific Results, **179**, 1–17.
- Naville, C., S. Serbutoviez, A. Throo, O. Vincké, and F. Ceconi, 2004, Seismic While Drilling (SWD) techniques with downhole measurements, introduced by IFP and its partners in 1990–2000: Oil and Gas Science and Technology, **59**, 371–403, doi: <https://doi.org/10.2516/ogst:2004027>.
- Poletto, F., M. Malusa, and F. Miranda, 2001, Numerical modeling and interpretation of drillstring waves: Geophysics, **66**, 1569–1581, doi: <https://doi.org/10.1190/1.1487102>.
- Poletto, F., and F. Miranda, 2004, Seismic while drilling: Fundamentals of drill-bit seismic for exploration: Elsevier.
- Poletto, F., F. Miranda, P. Corubolo, A. Schleifer, and P. Comelli, 2014, Drill-bit seismic monitoring while drilling by downhole wired-pipe telemetry: Geophysical Prospecting, **62**, 702–718, doi: <https://doi.org/10.1111/1365-2478.12135>.